Electrical Power and Energy Systems 94 (2018) 104–115

Contents lists available at ScienceDirect

Electrical Power and Energy Systems

journal homepage: www.elsevier.com/locate/ijepes

A blocking scheme for enhancement of distance relay security under stressed system conditions

Mohammad Sahand Parniani [a], Majid Sanaye-Pasand [a,*], Peyman Jafarian [b]

[a] School of Electrical and Computer Engineering, College of Engineering, University of Tehran, Tehran, Iran
[b] Transmission Grid Protection Office, Iran Grid Management Company (IGMC), Tehran, Iran

ARTICLE INFO

Article history:
Received 26 October 2016
Received in revised form 18 April 2017
Accepted 16 June 2017

Keywords:
Remote backup protection
Load encroachment
Power swing
Voltage decline
Zone-3 of distance relay

ABSTRACT

Mal-operation of zone-3 of distance relays has been one of the main causes of widespread disturbances and blackouts in power systems throughout the world. Under some non-faulty conditions, the measured impedance may enter zone-3 and cause spurious trip of transmission lines. This can happen during stressed system conditions such as power swing, extreme loading and voltage decline. In this respect, there is an essential need to improve security of zone-3. Introducing a new two-dimensional decision plane, this paper presents a new technique based on superimposed components of voltages magnitude to discriminate non-faulty conditions from fault events. This way, not only the rate of change of the voltage magnitude but also its pattern of change is included into the decision logic. The proposed method is able to provide high security and sensitivity in detecting non-faulty cases and prevents relay from undesired trip in such conditions. The 39-bus New-England test system is used to demonstrate the effectiveness of this method. The obtained results show that the proposed method is able to reliably distinguish stressed conditions from fault events for different power system disturbances and considerably improves security of distance relay.

1. Introduction

Distance protection schemes are conventionally designed so as to provide remote backup for all transmission lines (TLs) connected to the remote end to enhance reliability of the power network protection system. For this purpose, it is desirable to cover longest following line at the next substation by zone-3 of distance relays. Accordingly, reach of zone-3 of a distance relay might be extended close to the TL load limit. In such cases, it is likely that the impedance seen by the relay enters its operating characteristics under stressed system conditions, e.g. power swing, extreme loading condition, and voltage decline. This could lead to distance relay undesired operation and might result in cascading trips in the power system [1–4].

One of the main reasons of mal-operation of distance relays is load encroachment [5]. Under normal conditions, the distance relay mal-operation due to load encroachment can be prevented by reducing the reach of zone-3 [6]. Rather, numerical distance relays mostly provide a load encroachment element by which the relay trip is blocked if while the positive-sequence voltage is nearby the nominal value, the measured impedance is located inside a predefined load area. This way, the relay tripping characteristic is modified by excluding an load area corresponding to the maximum load with the highest power factor in the impedance plane [7–10]. Under extreme operating conditions of power system, however, the load impedance might enter the relay tripping zone and activate it, since such conditions are not commonly anticipated in the setting calculations. In [11], an adaptive anti-encroachment zone is proposed based on steady-state security analysis. The proper performance of this technique is highly dependent on communication system as it requires signals from the remote end to make a proper decision.

Dynamic encroachment of the measured impedance into the relay operating characteristics due to power swings subsequent to a disturbance can also cause spurious trip by distance relays. The conventional criterion used for identifying the power swing condition is based on the rate of change of apparent impedance seen by the relay [12–14]. Most of industrial relays use this criterion in some manner to differentiate between fault and power swing. In the GE D60 distance relay, the power swing condition is identified if the impedance locus spends more than a certain time between the outer and inner characteristics of the power swing blocking (PSB) function [8]. The ABB REL670 relay uses almost the same approach but since the initial swings are usually not as fast as the later swings, it employs a different timer for

* Corresponding author.
E-mail address: msanaye@ut.ac.ir (M. Sanaye-Pasand).

http://dx.doi.org/10.1016/j.ijepes.2017.06.020
0142-0615/

the consecutive swings [9]. In SIEMENS 7SA612 relay, the impedance vector calculated in 1/4 cycle intervals is monitored. If the change from one sample to the next is smaller than a predetermined value, and also not more than one of the two resistance and reactance components of the impedance vector (R, X) has changed its direction within one measuring window, the power swing is recognized [10]. However, finding appropriate settings for these algorithms need detailed stability studies for all possible power swing scenarios on the system which is not an easy task on a large power system [15].

In [16], it is shown that the resistance seen by the relay varies persistently during power swing condition whereas it is almost constant during fault events. However, recognizing power swings based on this feature requires long time to make an appropriate decision [17]. Jafari et al. [18] reported a scheme independent of the rate of change of power system parameters which is based on the locus of center of the admittance trajectory. Nonetheless, this scheme is not verified for zone-3 faults in which the center of admittance trajectory could be beyond the transmission line admittance characteristic. Using mathematical morphology (MM), a power swing detection method is proposed in [19] which detects swings by analyzing current waveforms and detects faults by analyzing voltage waveforms. But, the process of design and selection of structuring element in MM is very complex for application in a real power system. In [20], an algorithm based on the support vector machine (SVM) is proposed for discrimination between fault and power swing. Three phase current samples for half cycle duration of post-fault/power swing are given as an input to the SVM. However, the SVM classifier needs off-line training using a large data set to become capable of recognizing similar patterns under different conditions. Using both ends measurements, a data-mining based intelligent differential relaying scheme is proposed in [21] to provide supervisory control to the distance relays operation. This scheme is able to recognize power swing conditions within an acceptable time, but it is not a local technique. In [15] a method based on relative speed of a fictitious equivalent machine representing the entire system by its single machine infinite bus (SMIB) equivalent from the relay location has been proposed to discriminate stable power swings from unstable ones. If the relative speed goes through a zero crossing, the swing is classified as a stable power swing, otherwise it is classified as an unstable swing. But, this method requires a long time to make decision and also it does not block the distance relay during unstable power swings.

Voltage instability has been identified as one of the main reasons for most of the recent power systems blackouts worldwide. Under stressed voltage conditions, the voltage magnitude reduces in most of the buses and consequently, the impedance seen by the relay decreases. As a result, the measured impedance might enter zone-3 of distance relays and cause undesired TL tripping. In [22], an adaptive algorithm based on the rate of change of voltages magnitude is proposed to distinguish voltage instability from fault events and prevent zone-3 mal-operation. In [23], it is proposed to use the rate of change of currents magnitude as well, to make the algorithm more secure. But, this could make the algorithm more susceptible to mal-operation during switching large loads in which line current increases suddenly. Also, it cannot detect power swing condition and an additional algorithm is required to provide power swing blocking. In [24], a voltage stability index is proposed to detect stressed voltage condition and block the relay operation. Nikolaidis [25] proposed to modifies the zone-3 characteristic if some predefined conditions are fulfilled, indicating that a severe system situation is evolving. This method detects the voltage stressed condition based on the rate of change of apparent impedance during the transition between two supervisory zones. But, finding proper setting for the supervisory zones of all distance relays in a bulk power system needs detailed dynamic studies and is extremely tedious.

In [26], a method based on wide area measurement system (WAMS) is proposed in which critical relays that are prone to undesired operation are identified using state estimation, and then wide area control is used to block these relays. In [27], a synchrophasor-based wide area backup protection is presented which detects faults by comparing the calculated voltage of each bus from more than one path. In [28], a fuzzy logic based method combining different indices including angle, frequency, voltage and damping information derived from WAMS data is used to prevent mal-operation of relay during power swing condition. The intelligent scheme proposed in [29], called online sequential extreme learning machine (OSELM), blocks zone-3 during voltage instability and also power swing conditions. This method needs data from different PMUs installed in the transmission network to work properly. Although WAMS based approaches can help to achieve a secure backup protection, their reliable performance is highly dependent on reliability of the communication system. Therefore, depending on placement of measurement units, they may fail to operate correctly if some of the measurement units are disconnected from the control center.

This paper introduces a new simple and powerful technique for enhancing security of distance relay zone-3 using local measurements. In order to distinguish fault events from stressed system conditions, a two-dimensional decision plane is proposed which uses the superimposed voltages magnitudes. The fault occurrence is identified based on the trajectory of samples of defined indices in this plane. This way, the change in the voltage during two subsequent cycles is observed simultaneously. Accordingly, not only the rate of change of the voltage magnitude but also its pattern of change is incorporated into the decision making logic, which helps to provide higher sensitivity and reliability in discrimination of fault events. The proposed technique is evaluated using the 39-bus New-England test system for different power system events. The obtained promising results show that the proposed technique is well capable to discriminate between faulty and non-faulty conditions and can enhance security of distance relay zone-3 operation during stressed system conditions.

2. The proposed technique

2.1. Proposed discrimination feature

For a given signal $x(t)$ sampled at the frequency of $f_s = N \cdot f$, the superimposed component can be defined as follows [30–32]:

$$\Delta x(n) = x(n) - x(n-N) - [x(n-N) - x(n-2N)] \quad (1)$$

where $x(n)$ is the measured signal sampled at instant n, N is the number of samples per cycle, and f is the power frequency. Therefore, $x(n-N)$ and $x(n-2N)$ are the signal samples measured one cycle and two cycles earlier than the instant n, respectively.

The proposed algorithm is based on the superimposed voltages magnitudes which are obtained using discrete Fourier transform (DFT) algorithm. The above equation can be rewritten as follows:

$$\Delta|v(n)| = |v(n)| - |v(n-N)| - [|v(n-N)| - |v(n-2N)|] \quad (2)$$

$$\Delta|v(n)| = -k_1 + k_2 \quad (3)$$

where k_1 and k_2 are defined as

$$k_1 = |v(n-N)| - |v(n)| \quad (4)$$

$$k_2 = |v(n-2N)| - |v(n-N)| \quad (5)$$

The indices k_1 and k_2 are used in the proposed algorithm to construct a two-dimensional decision plane for discrimination between faulty and non-faulty conditions. Since k_1 and k_2 correspond to the change of signal during one cycle interval, the rate of change of voltage is implicitly included into the decision logic. Using the trajectory pattern of the defined indices in the proposed two-dimensional plane, fault events can be well distinguished from non-faulty stressed conditions. The following subsections illustrate the distinctive feature of each event by which the proposed algorithm recognizes fault events from stressed conditions and blocks/unblocks operation of the distance relay zone-3.

2.2. Distinctive feature of fault event

During normal condition, both of the k_1 and k_2 indices are almost zero. When a fault occurs, the voltage magnitude of the faulty phases would decrease rapidly. As a result, k_1 increases to a positive value as soon as a fault occurs while k_2 remains almost zero until one cycle after the fault occurrence instant. Then after, the value of k_2 starts to increase while the value of k_1 starts to decrease.

A simple transmission system used for the preliminary simulations is considered in Fig. 1. The value of the defined indices for occurrence of a three-phase fault on this transmission system is shown in Fig. 2. The full-cycle DFT is employed to extract the voltage fundamental frequency component. As a result, k_1 increases smoothly after the fault instant and reaches to its final value after one cycle when all pre-fault samples are removed from the data window. Then, it starts to decrease smoothly and reaches to zero after two cycles. As can be seen, the pattern of k_2 is similar to that of k_1 but it starts to increase one cycle after the fault instant. Fig. 2 (c) depicts the difference between the indices k_1 and k_2. As can be observed, for a short circuit fault, the value of $k_1 - k_2$ is equal to k_1 during the first cycle after the fault instant. The value of $k_1 - k_2$ becomes negative after almost two cycles and returns to zero three cycles after the fault instant. The value of $k_1 + k_2$ is also depicted in Fig. 2(d).

2.3. Distinctive feature of power swing condition

During a power swing, the power flow between two areas of the system oscillates due to fluctuation of the relative voltage phase-angle between an electrical machine or a group of machines and the power system voltage source. The power swing is observed at the relay location as deviation of the power system frequency from its nominal value and fluctuation of magnitudes of voltages and currents waveforms.

For a slow power swing, the change of voltage during one cycle is negligible, and hence the value of k_1 is small. As shown in Fig. 3, by using an appropriate threshold (TH1) for detection of fault events, such slow swings do not exceed the threshold and can be well distinguished from short circuit faults. For fast power swings, however, the amount of the change of voltage during one cycle might be considerable. This is not only because of fluctuation of the voltage magnitude, but also due to the change of the frequency of voltage waveform. This could cause the index k_1 to exceed the threshold TH1 especially at voltage zero-crossing points. Indeed, most of the methods proposed for power swing detection encounter difficulty during fast power swings.

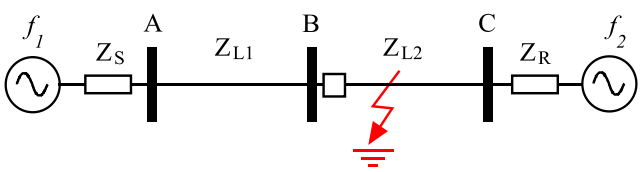

Fig. 1. Simple transmission system used for preliminary simulations.

It is worth noting that unlike a fault event, during a power swing, the index k_2 is not zero when k_1 exceeds TH1 and its value at this point is nearly equal to k_1. Accordingly, the difference between these two indices $(k_1 - k_2)$ would be smaller than TH1, as can be observed in Fig. 3(c). Conversely, in the case of fault events, the value of $(k_1 - k_2)$ is equal to k_1 when k_1 exceeds the threshold. Therefore, the first criterion to recognize a fault event is defined as follows:

$$if\ (k_1 > TH_1 \,\&\, k_1 - k_2 > TH_1) \Rightarrow Fault\ Event \tag{6}$$

Fig. 3 depicts the values of the defined indices during power swings with two different frequencies. To simulate power swing condition in the simplified system shown in Fig. 1, the frequency of the left hand side source (f_1) is considered to be greater than 50 Hz while the frequency of the other source (f_2) is fixed at 50 Hz. As can be seen, for a 2 Hz power swing, the value of k_1 is smaller than the threshold TH1. By increasing the frequency of power swing, k_1 exceeds TH1 when the swing frequency is considered to be 6 Hz. Desirably, as can be observed in Fig. 3(b), the value of k_2 is not zero when k_1 passes TH1, and therefore $(k_1 - k_2)$ is smaller than the threshold TH1. Thus, it can be confirmed that the power swing condition would be properly distinguished from the fault event by the proposed criterion given in (6).

2.4. Distinctive feature of load encroachment and stressed voltage conditions

When a fault occurs in a power system, the voltage drops rapidly at the fault point. Consequently, voltage magnitude measured by the relay changes significantly in the faulty phases at the fault occurrence instant. On the contrary, during load encroachment and stressed voltage conditions, the change of voltage is small during each cycle. In [23] and [22], a method based on calculating the derivative of voltage has been proposed to discriminate between fault and non-faulty conditions. It can be described as follows:

$$\begin{cases} \frac{\Delta V}{\Delta t} \leqslant Threshold \Rightarrow No\ Fault \\ Otherwise \Rightarrow Fault\ Event \end{cases} \tag{7}$$

As in this paper, the value of Δt is fixed and it is equal to one cycle of the power frequency, the criterion given in (7) can be rewritten as follows:

$$if\ (k_1 < TH_2) \Rightarrow No\ Fault \tag{8}$$

In fact, the criterion in (8) corresponds to the rate of change of voltage magnitude during one cycle.

2.5. Distinctive feature of low voltage drop faults

In the case of low voltage drop faults, change of voltage magnitude might be small. This situation happens when a high resistance fault occurs or the value of source impedance ratio is low, especially when the fault is located at the end of zone-3. In this condition, the amount of change of the voltage might be less than TH1 and thus, the criteria given in (6) would not be satisfied. However, if the threshold TH2 is appropriately adjusted, the value of k_1 would become greater than this threshold and therefore, such faults can be distinguished from load encroachment and stressed voltage conditions. For these faults, the index k_2 is nearly zero when k_1 exceeds the threshold TH2. As a result, the value of $(k_1 - k_2)$ is almost equal to k_1 at this condition while it is smaller

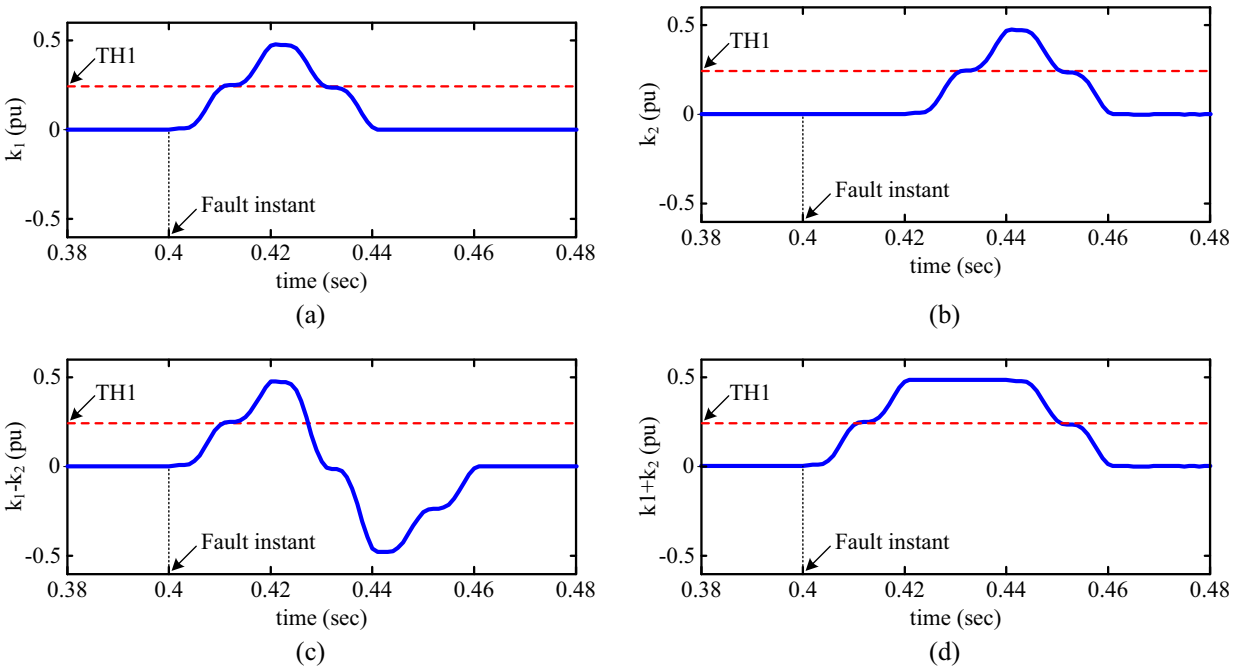

Fig. 2. Value of the defined indices calculated for a three-phase fault, (a) k_1, (b) k_2, (c) k_1-k_2, (d) $k_1 + k_2$.

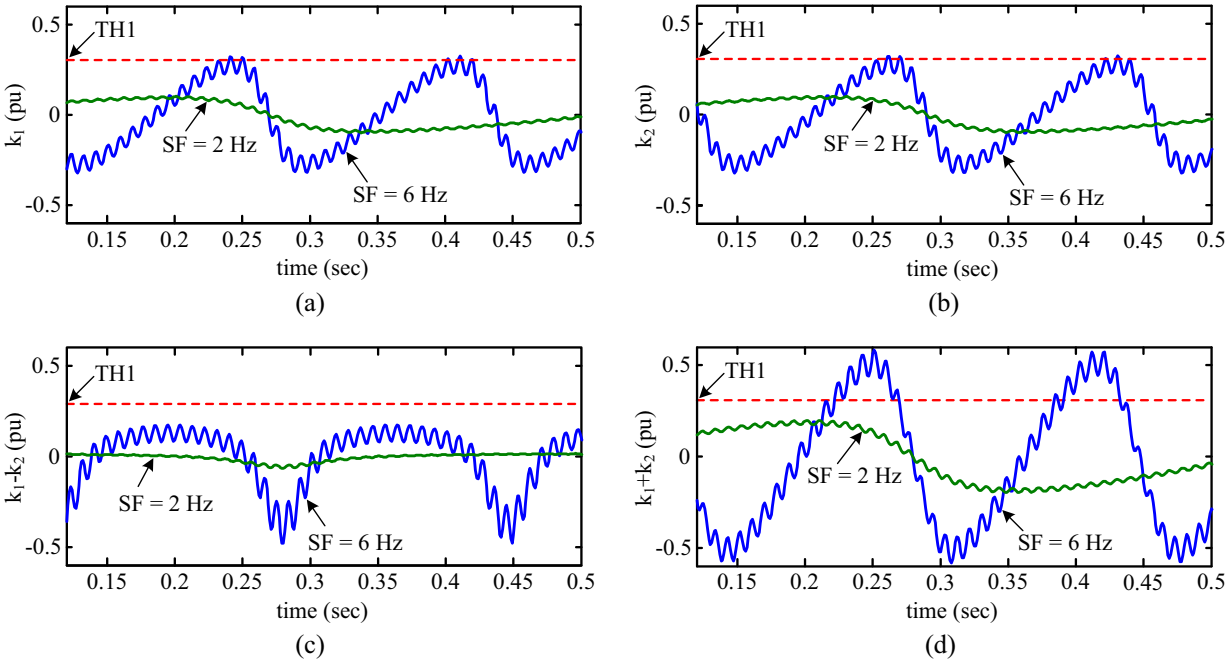

Fig. 3. Value of the defined indices calculated for two slow and fast power swings, (a) k_1, (b) k_2, (c) $k_1 - k_2$, (d) $k_1 + k_2$.

than the threshold for non-faulty conditions especially in the vicinity of voltage collapse. This criterion can be written as follows:

$$if\ (k_1 - k_2 < TH_2) \Rightarrow No\ Fault \tag{9}$$

As can be seen in Fig. 2, the maximum value of $(k_1 + k_2)$ is almost equal to the maximum value of k_1 for the fault case. Therefore, if for a low voltage drop fault, the value of k_1 is smaller than TH1, the value of $(k_1 + k_2)$ at any instant, would be smaller than this threshold as well. So, another criterion is defined as follows:

$$if\ (k_1 < TH_1 \,\&\, k_1 + k_2 > m * TH_1) \Rightarrow No\ Fault \tag{10}$$

where m is a constant factor greater than one used to make the criterion more secure to ensure that measurement errors do not cause incorrect decision during a fault case when the maximum value of k_1 is very close to TH1 but smaller than that.

2.6. The proposed two-dimensional decision plane

The criteria given in (6)–(10) can be described by the two-dimensional decision plane shown in Fig. 4. For example, criterion (6) forms area C in this plane. When a fault occurs, the index k_1 starts to increase immediately. Thus, trajectory of the indices k_1

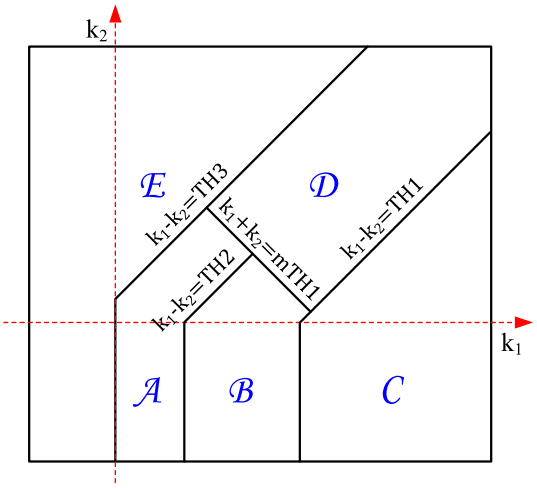

Fig. 4. The proposed two-dimensional decision plane.

and k_2 begins from area A and then enters area C. If the samples have entered area C, the algorithm would conclude that a fault has occurred and issues an unblock command. In the case of non-faulty conditions such as load encroachment, trajectory of the defined indices remains in area A and the proposed algorithm concludes that no fault has occurred. In addition, if the samples have entered area D, a fast power swing would be recognized.

It should be noted that for the cases in which none of the criteria given in (6)–(10) are satisfied, trajectory of the indices enters area B but does not enter area C. This situation happens when a low voltage drop fault has occurred. Similarly, for a fast power swing, the samples may pass area B before entering area D. Thus, it is not possible to decide whether it is a low voltage drop fault or a power swing only based on locating the samples in area B. In the case of a low voltage drop fault, trajectory of the indices enters area B and without entering area D, this trajectory crosses area A and the line $k_1 - k_2 = \text{TH3}$, and then it will enter area E after a while. So, when trajectory of samples enters area B, the algorithm would wait till the trajectory has entered area E. If before entering area E, trajectory has entered area D, a fast power swing is identified, otherwise it is concluded that a low voltage drop fault has occurred. It should be pointed out that this decision plane is formed for every three phases of voltage signals. So only for the faulty phases, the fault is concluded in its related plane.

Fig. 5 shows trajectory of the defined indices in the proposed decision plane for a three-phase fault and also a fast power swing in the system shown in Fig. 1. It begins from the origin at $k_1 = k_2 = 0$ and moves towards the right and after a short time, it eventually returns back towards the origin. The values of TH1, TH2 and TH3 are respectively set to 20%, 10% and −8% of the nominal voltage and the safety factor m is set to 1.2. As observed in Fig. 5(a), for the fault case, trajectory of the defined indices enters area C. For the power swing case shown in Fig. 5(b), the trajectory enters area B, meanwhile before entering area E, it first enters area D, and thus a non-fault condition is concluded.

2.7. Flowchart of the proposed algorithm

The proposed algorithm is implemented by two parallel running subroutines. The first one, which is continuously executed in the background, calculates the superimposed components and determines the position of the defined indices in the proposed decision plane. For each new relay input sample, if the area in which the defined indices are located is different from that of the previous sample, the new area is stored to the top of a buffer. The second subroutine is executed only if the impedance trajectory has entered the distance relay operating zone, to determine whether a fault has occurred or not. If yes, the distance relay trip would be unblocked. To do so, the position of the defined indices determined and stored in the buffer by the parallel subroutine, is used to make a decision.

The flowchart shown in Fig. 6 starts when the relay is switched on. Tripping of distance relay zone-3 is blocked unless a fault is identified by the proposed algorithm. At the moment of entrance of the impedance trajectory into the zone-3 of distance relay and as long as the impedance locus lies inside the zone-3, the second subroutine is executed, and it would be checked to determine if the defined indices k_1 and k_2 have entered the specified area C or not. If the defined indices have entered this area, a fault would be identified and zone-3 trip would be unblocked. If no sample has entered area C but the indices have entered area B, the proposed method waits until the samples move into area E of the decision plane. During this interval, the first subroutine is being performed in parallel in the background as a new sample becomes available. As illustrated previously, for the power swing condition, the trajectory would pass area D before entering area E. Thus, if before entrance of the define indices into area E, they have not entered area D, it would be concluded that a fault has occurred.

2.8. Threshold selection

The threshold TH1 should be chosen in such a way that the values of k_1 and $k_1 - k_2$ exceed this threshold only for definite fault events, making sure that the fastest feasible power swing in the system and severe non-fault voltage drops do not cause an undesired unblock. Compared to the existing techniques which are based on the rate of change of voltage magnitude, the proposed two-dimensional decision plane permits to use a higher value for TH1 since it is not necessary to simultaneously cover low voltage drop faults by this stage.

The threshold TH2 should be chosen to distinguish low voltage drop faults from load encroachment and stressed voltage conditions. The lower the threshold TH2 is set, the faults with lower voltage drops could be covered by the proposed algorithm. Nonetheless, distinguishing voltage drops during non-faulty system disturbances such as an equipment outage would become more difficult. On the contrary, a higher value for TH2 provides higher security, but the coverage of low voltage drop faults would be reduced.

The threshold TH3 is used to form area E in the decision plane, and should be chosen so as to ensure that during a fast power swing, trajectory of samples of the defined indices does not move directly from area B into area E without passing area D. Meanwhile, it should be considered that this threshold should not be greater than TH2, in order to make sure that the trajectory enters area E after it has entered area B during a low voltage drop fault. Based on various simulation studies, an appropriate value for TH3 is to set it nearly equal to the absolute value of TH2 with a negative sign.

In the event of low voltage drop faults, trajectory of the defined indices would enter area B without entering area C. Then after, it directly moves into area E and consequently, the fault would be recognized. Otherwise, if some samples are located inside area D, it would be concluded that a power swing has occurred. The safety factor m is used to ensure that measurement errors and transients generated during the fault do not cause the trajectory of defined indices to enter area D, averting the proposed method from wrong decision.

Indeed, the amount of voltage drop at a transmission network bus depends on the network operating condition and topology,

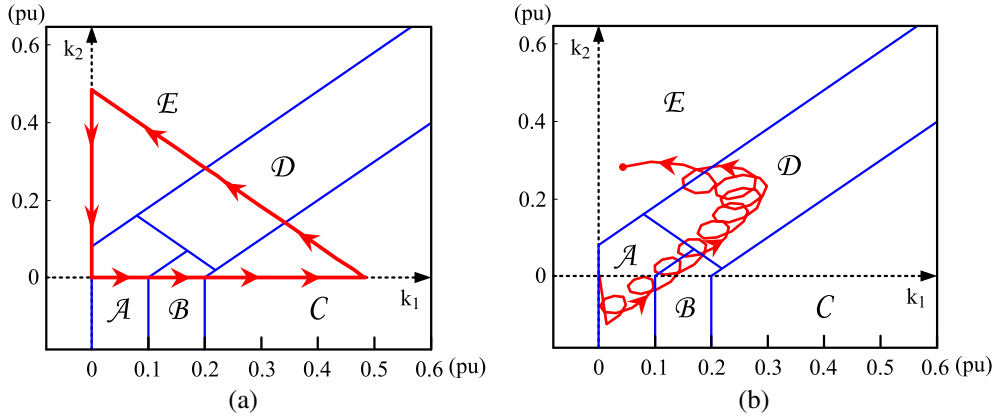

Fig. 5. Trajectory of the defined indices in the proposed two-dimensional decision plane, (a) for a short circuit fault, (b) for a fast power swing at frequency of 6 Hz.

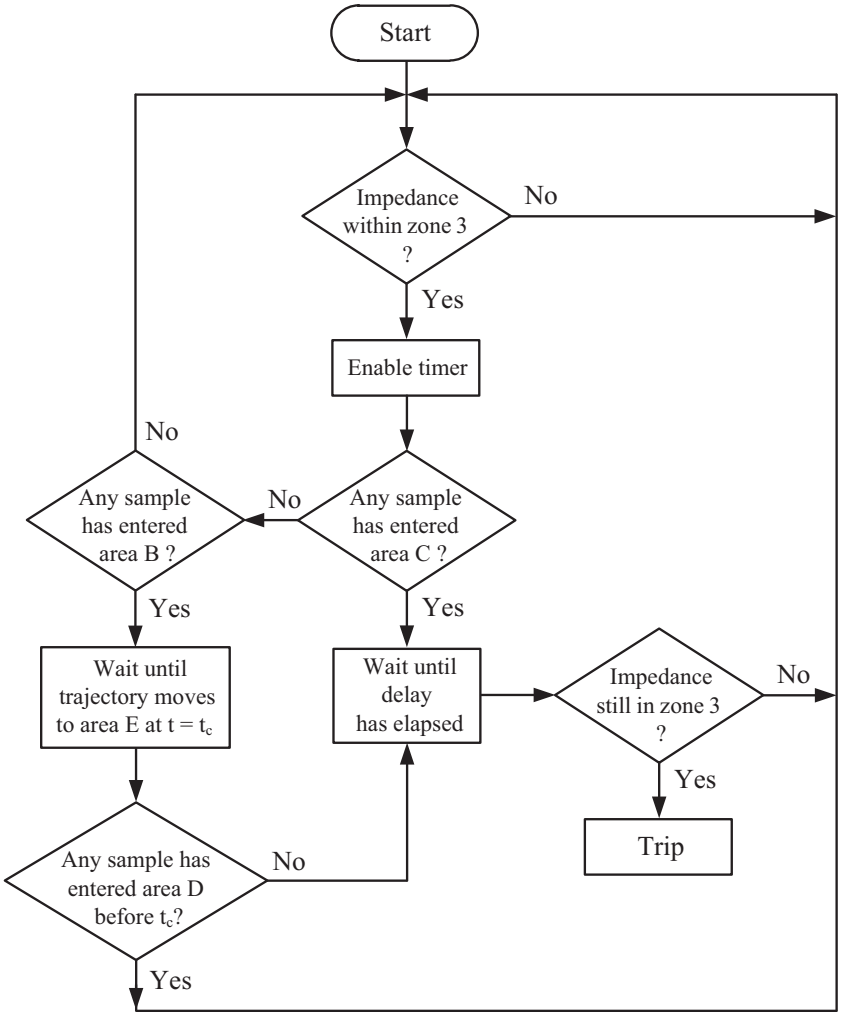

Fig. 6. Flowchart of the proposed algorithm.

or in brief, the bus stiffness. Thus, to ensure that the proposed algorithm is able to recognize fault events reliably under all possible operating conditions, it is required to set the thresholds TH1 and TH2 for the worst condition which corresponds to the maximum stiffness of the bus. Meanwhile, since variation of the system inertia could change the power swing frequency, the fastest power swing condition should be used in setting calculations. In the IEEE 39-bus test system benchmark, based on extensive simulation studies, we have found out that by using the voltage signal, it is possible to reliably discriminate fault events under different operating conditions. However, for a rare transmission system in which there is a considerable difference between the maximum and

minimum short circuit levels, it might be better to use a combination of voltage and current signals. Under the maximum short-circuit level condition, due to small network Thévenin impedance, the amount of the voltage drop at the fault moment would be smaller than that under the minimum short-circuit level. But, the change in the current would be larger. Thus, a combination of these two signals could help to make the algorithm more robust against changes in the network.

3. Simulation studies

In this study, the 39-bus test system [33] provided in Appendix A is used to evaluate the proposed algorithm performance. Extensive simulations including low impedance faults, high impedance faults, power swing, load encroachment and equipment outages are carried out using DIgSILENT software [34]. The effect of transients of capacitive voltage transformers (CVTs) on performance of the algorithm is also studied in this paper. In order to implement the proposed algorithm, the obtained signals are recorded and are transferred to another appropriate software. The measured signals are first passed through a second-order antialiasing Butterworth filter with a cutoff frequency of 400 Hz, and then the DFT algorithm is used to estimate the fundamental component of voltage signals. The sampling frequency used in the DFT calculations is considered to be 1 kHz. Based on extensive simulation studies, the thresholds TH1, TH2, and TH3 of the relay R_1 located at bus 29 protecting line 29-28 are respectively set to 10%, 20%, and −8% of the nominal voltage, and the safety factor is set to 1.2.

3.1. Fault event

Many simulation studies are carried out to investigate the proposed algorithm performance in discrimination of fault events. Due to space limit, only the results obtained for a 1-ph-g fault on bus 26 is presented here, as an example. Fig. 7 depict trajectory of the defined indices seen at bus 29 by relay R_1. As can be seen, in the case of low impedance fault, the trajectory enters area C and hence, the fault is identified immediately. In the case of high impedance fault, the trajectory enters area B, and after a short time, it moves towards area E, without entering either areas C or D. Therefore, in both cases, the fault is correctly recognized. It should be noted that high voltage drops corresponding to low impedance faults are identified in less than one cycle. But low voltage drop faults (in this case high impedance faults), require a longer time of about 2 cycles to be recognized. Nevertheless, this time is still negligible compared to operation time of the distance relay zone-3.

3.2. Load encroachment

During extreme loading conditions, the impedance measured by a distance relay might enter its operating characteristics. It is quite important that the relay discriminates load encroachment from short circuit faults in order to avoid spurious tripping of a transmission line and subsequent cascading trips.

To simulate load encroachment into zone-3 of relay R_1, load on bus 28 is gradually increased in six steps with the time intervals of 1 s. The amount of increased load at each step is considered to be 30% of the total load on bus 28. Fig. 8(a) shows the impedance measured by relay R_1. The trajectory of samples of the defined indices in the proposed two-dimensional decision plane is depicted in Fig. 8(b). It is observed that during load encroachment, the trajectory remains in area A, and hence the proposed algorithm is able to prevent the relay mal-operation.

3.3. Power swing

In this section the performance of the proposed algorithm during a stable power swing and an unstable power swing is investigated.

3.3.1. Stable power swing

In this case, a three-phase fault is simulated at t = 0.3 s on the middle of line 29-26. This fault is cleared after 600 ms by isolating the faulted line. Consequently, power swing occurs in the system and the measured impedance enters zone-3 of relay R_1 as shown in Fig. 9(a). As the impedance remains in zone-3 for more than the time setting of this zone, it can result in relay mal-operation. As shown in Fig. 9(b), trajectory of the defined indices moves within area A and opposite side of the proposed two-dimensional decision plane and enters neither areas B nor C. Accordingly, the proposed algorithm correctly prevents the relay from mal-operation.

3.3.2. Unstable power swing

In this case, a three-phase fault is simulated on line 29-26 at t = 0.3 s, and it is cleared after 1.2 s. The delayed fault clearance results in an unstable power swing in the system. The impedance measured by relay R_1 is plotted in Fig. 10(a). In this case, the measured impedance enters zone 2 as well as zone-3 of relay R_1. The frequency of swings in the voltage waveform of bus 29, reaches to about 7 Hz at the third swing cycle. Fig. 10(b) depicts the trajectory of samples of the defined indices in the proposed two-dimensional plane. As can be seen, since the swing frequency is high, the trajectory enters area B. However, as samples enter area

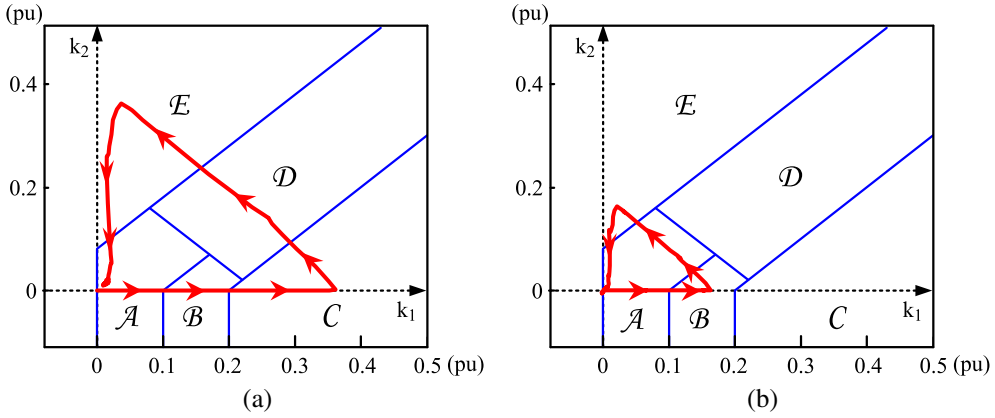

Fig. 7. Trajectory of the defined indices for a 1-ph-g fault, (a) $R_f = 0$, (b) $R_f = 30\ \Omega$.

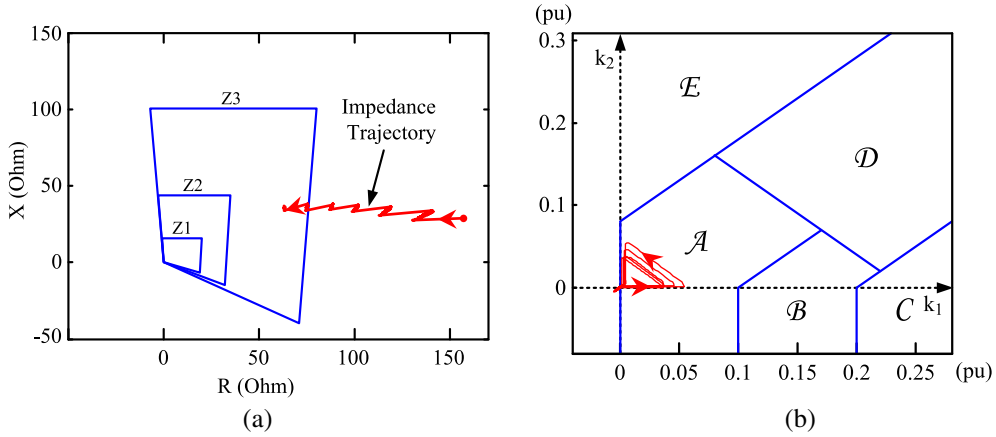

Fig. 8. Obtained results during load encroachment, (a) impedance seen by relay R_1, (b) trajectory the defined indices.

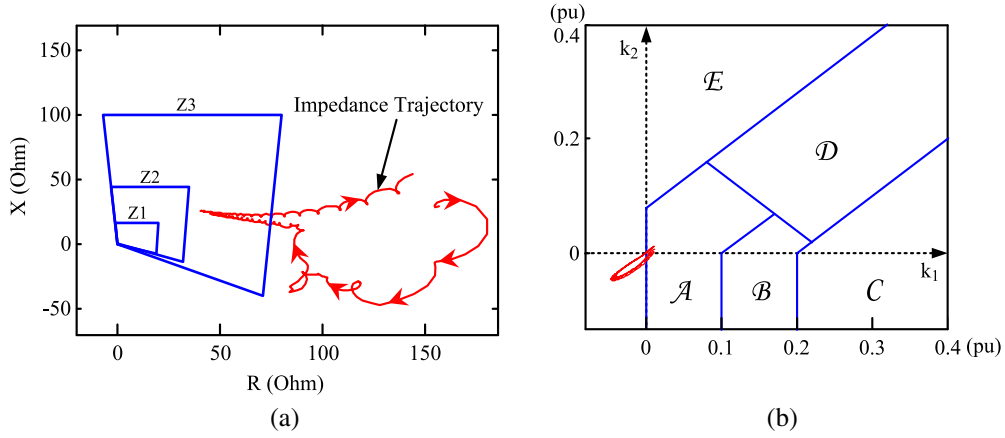

Fig. 9. Obtained results for the stable power swing, (a) impedance trajectory seen by relay R_1, (b) trajectory of the defined indices.

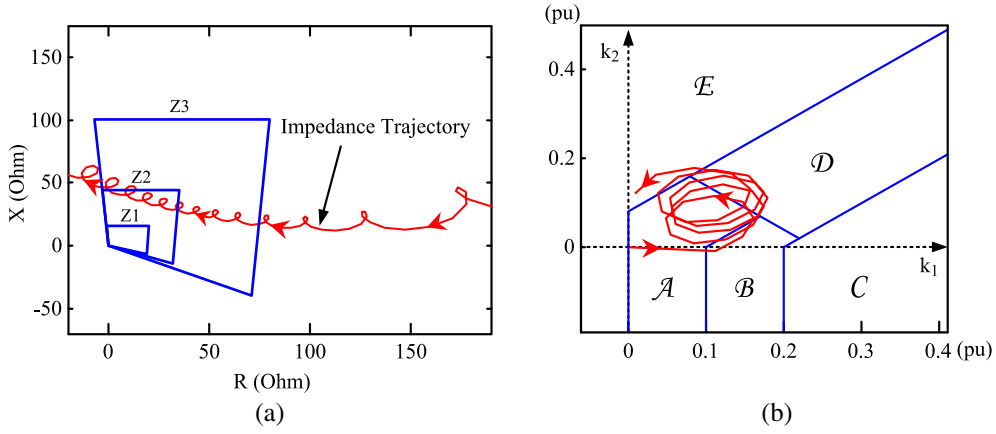

Fig. 10. Obtained results for the unstable power swing, (a) impedance trajectory seen by relay R_1, (b) trajectory of the defined indices.

D before entering area E, the fast power swing is well identified. It can be concluded that the proposed algorithm is able to correctly detect slow and fast power swings and discriminate swing conditions from fault events.

3.4. Equipment outage

In the case of outage of an equipment, e.g. transmission line, generator or transformer, the voltage of different buses would be reduced which may cause the measured impedance enter zone-3 of a distance relay. The proposed method should detect these events and prevent undesirable relay trip. To demonstrate the proposed method performance during equipment outage, generator 8 and also line 29-26 are disconnected one by one.

The obtained results for these two events are depicted in Fig. 11(a) and (b). As shown, the trajectory of the defined indices remains in area A and enters neither areas B nor C. As a result, the proposed method concludes that no fault has occurred and blocks the relay correctly.

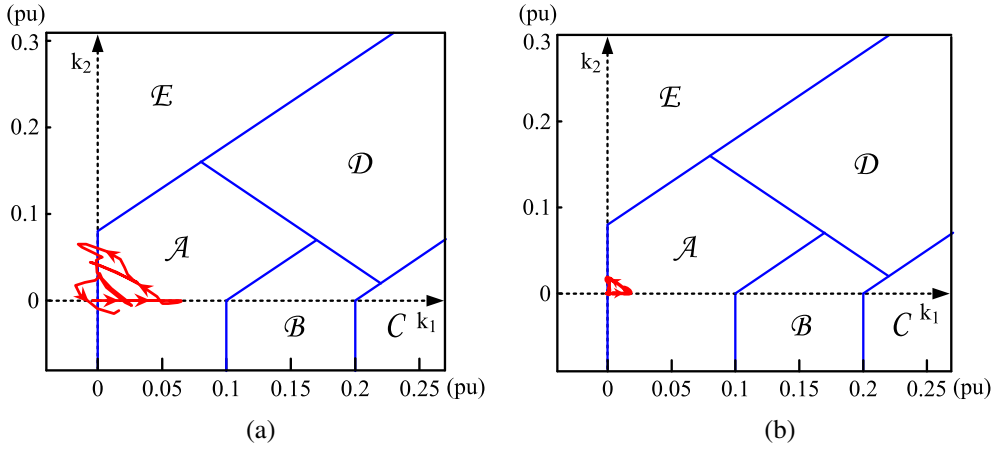

Fig. 11. Trajectory of the defined indices, (a) during generator 8 outage, (b) during transmission line 29-26 outage.

3.5. Influence of CVT transients

Following a voltage drop in the system, the secondary voltage of CVT might not be an exact replica of its primary side for a transient period. The larger the voltage drop at the relay location, the larger the CVT transients. Thus, since the proposed algorithm is based on the voltage signal, it is necessary to investigate influence of CVT transients on its performance. For this purpose, two faults with different amounts of voltage drops are simulated on line B-C of the system shown in Fig. A.

Fig. 12 shows trajectory of the defined indices for these two cases. As shown, when voltage drop is high, samples enter area C of the decision plane and the fault is identified immediately irrespective of high CVT transients. Also when voltage drop is small, trajectory of samples enters area B. In the latter case, the CVT transient is small and hence, its influence on trajectory movement is negligible. The trajectory moves towards area E without entering area D and the proposed algorithm recognize the fault correctly. Therefore, the transient of CVT does not have any influence on performance of the proposed method.

3.6. Power system frequency drift

To evaluate the proposed algorithm performance under drift in the power system frequency from its nominal value, a number of simulations are performed. The obtained results for the worst condition in which the power system frequency is decreased to 48 Hz are presented in Fig. 13. As can be seen, although there is no fluctuation in the voltage waveform, its corresponding superimposed components (k_1 and k_2) are not zero. This is due to the fact that the sampling frequency is considered to be constant (1 kHz), which is equivalent to 20 samples per cycle for a 50 Hz signal. As a result, the data-window length is not exactly equal to one cycle of the input signal, resulting in leakage error in estimation of the signal fundamental component. Since the superimposed components are obtained by subtracting the voltage magnitude estimated at any given instant from that estimated 20 samples earlier, the frequency drift will cause error in the calculations. However, as shown in Fig. 3, both k_1 and k_2 remain below the set thresholds. Accordingly, as can be seen in Fig. 14, trajectory of the defined indices remains inside area A of the proposed two-dimensional plane, indicating that this condition is not incorrectly detected as a fault event by the proposed algorithm.

3.7. Comparative assessment

In this section, the performance of the proposed algorithm is compared with that of the existing methods presented in [4], [22], and also the conventional PSB technique. These methods are compared in response to different power system events.

In [4], a new method is presented to discriminate three-phase faults from other non-faulty conditions. This method uses two criteria. The first criterion is the magnitude of current signal transients that should be more than a predefined value, and the second one is the angle of positive sequence impedance measured by the relay that should be more than a predefined threshold as

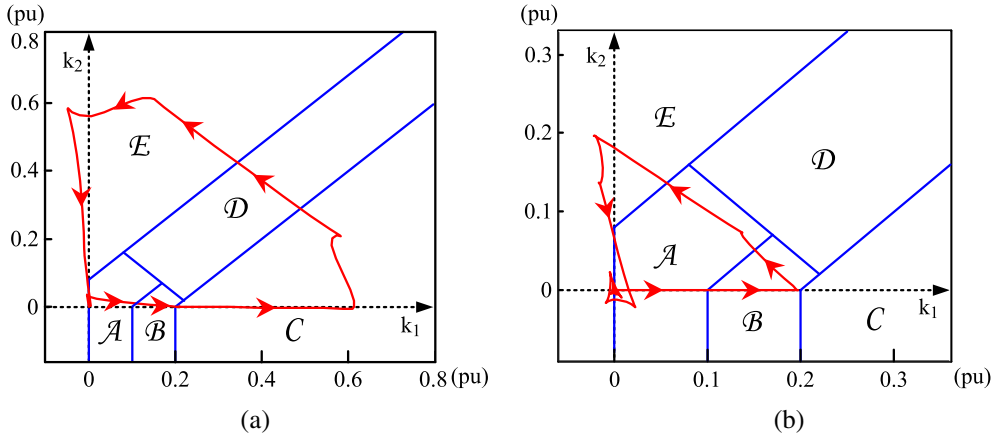

Fig. 12. Trajectory of the defined indices from CVT output, (a) during a high voltage drop fault, (b) during a low voltage drop fault.

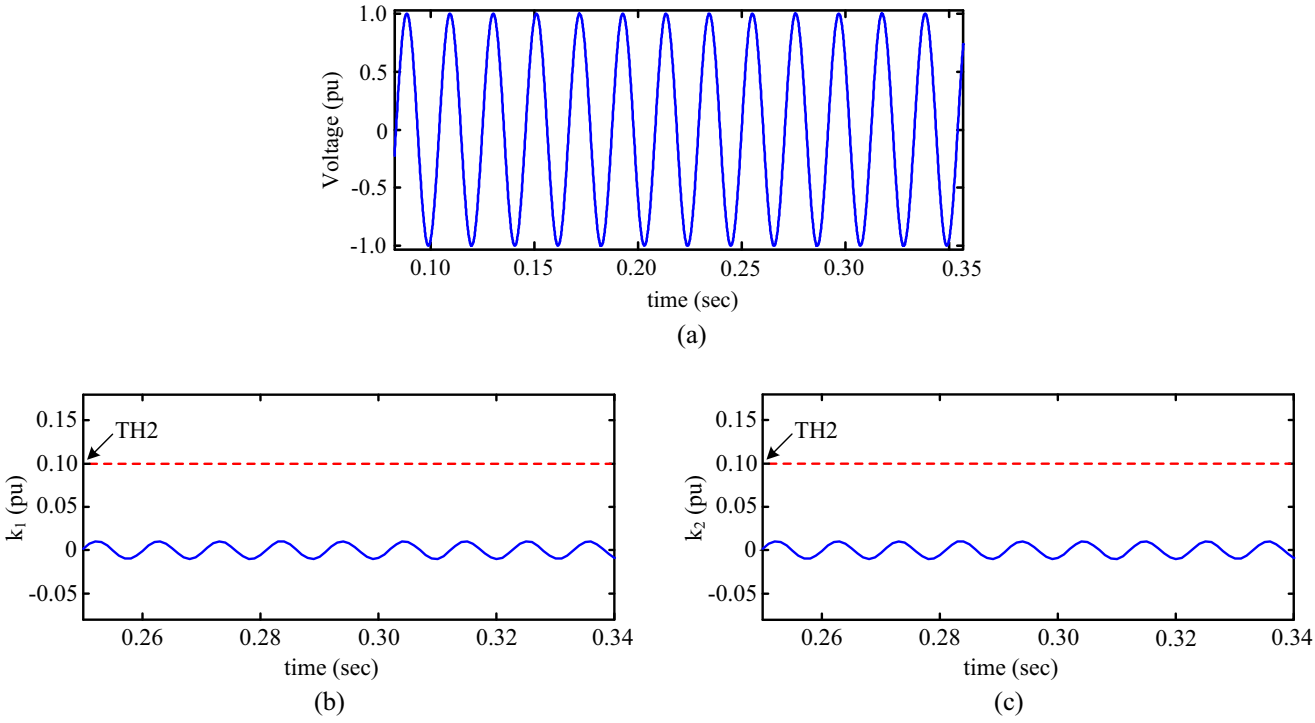

Fig. 13. Obtained results for power system frequency drift, (a) voltage waveform (b) k_1, (c) k_2.

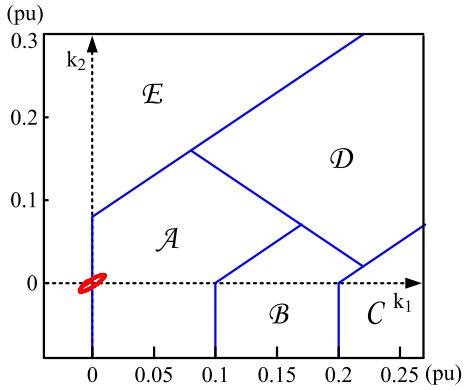

Fig. 14. Trajectory of the defined indices for the case of drift in the power system frequency.

well. If these two criteria are satisfied, a fault would be detected. In [22], derivative of voltage signal is used to detect fault from non-faulty cases. In this method if derivative of the voltage signal exceeds a predefined value, occurrence of a short circuit fault is concluded. The conventional PSB method employed in industrial distance relays uses a zone called power swing detection (PSD) zone. Based on the time interval that the impedance trajectory travels between borders of the PSD zone, it is concluded that a power swing and/or a fault condition has occurred, and the relay trip is blocked in the case of power swing.

Table 1 presents the results obtained by the proposed algorithm and that of the above mentioned methods for different power system incidents, such as load encroachment, power swing, generator and line outages and short circuit fault. In this table, the superscript (∗) indicates relay mal-operation. As can be seen from the table, in most cases, the conventional method would operate incorrectly and hence undesirable tripping would occur. Since the method explained in [4] does not consider single-phase-to-ground (1-ph-g) faults, such faults are not considered for evaluation of this method. Also, this method encounters difficulty in distinguishing fast power swings from three-phase faults, because during a fast power swing, the rate of change of the current magnitude in one cycle is large. Indeed, this method correctly distinguishes different stressed conditions such as load encroachment and equipment outages from three-phase faults. The method explained in [22] provides similar performance to the proposed algorithm under stressed voltage condition. This method, however, cannot distinguish power swing from short circuit faults, since it only uses the change of voltage magnitude during one cycle, and

Table 1
Results obtained by various methods for different power system events.

Description	Conventional method	Method proposed in [4]	Method proposed in [22]	Proposed method
Generator 8 outage	Trip*	Block	Block	Block
30% sudden increase in load 28	Trip*	Block	Block	Block
1-ph-g fault, $R_f = 0\ \Omega$	Trip	–	Trip	Trip
1-ph-g fault, $R_f = 20\ \Omega$	Trip	–	Trip	Trip
1-ph-g fault, $R_f = 40\ \Omega$	Trip	–	Trip	Trip
Three-phase fault	Trip	Trip	Trip	Trip
Line 29-26 outage	No entrance into zone-3	No entrance into zone-3	No entrance into zone-3	No entrance into zone-3
Slow power swing	Block	Block	Trip*	Block
Fast power swing	Trip*	Trip*	Trip*	Block

* Indicates relay mal-operation.

as was shown in Section 2.3, the amount of change in voltage magnitude during each cycle could be significant for the case of fast power swings. Since the proposed algorithm uses the change of voltage magnitude in two subsequent cycles, and by virtue of the two-dimensional decision plane, discrimination between fault events and stressed conditions has been improved significantly.

The proposed method in this paper not only distinguishes stressed voltage conditions such as load encroachment and equipment outages from different types of faults, but also is able to detect power swings even with high swing frequencies. In contrary to the previously proposed algorithms, it can detect both of the high and low voltage drop faults.

4. Conclusion

One important issue of distance protection scheme is to distinguish fault events from non-faulty disturbances such as power swing, load encroachment and stressed voltage conditions in order to make zone-3 of distance relays more secure and reliable. This paper proposed a new method based on superimposed components of voltage signal in a two-dimensional decision plane to distinguish fault events from the non-faulty ones. Monitoring trajectory of superimposed components of voltage magnitude in this plane, the proposed algorithm not only includes the rate of change of the voltage magnitude but also its trajectory pattern into the decision logic. The proposed algorithm performance was evaluated for various power system events, and also it was compared with some existing methods. The obtained results demonstrate that the proposed algorithm can well and reliably distinguish faults from non-faulty disturbances.

Acknowledgement

This work was supported by the University of Tehran under Grant No. 8101064-1-10.

Appendix A

Fig. A illustrates the single line diagrams of the simulated transmission system.

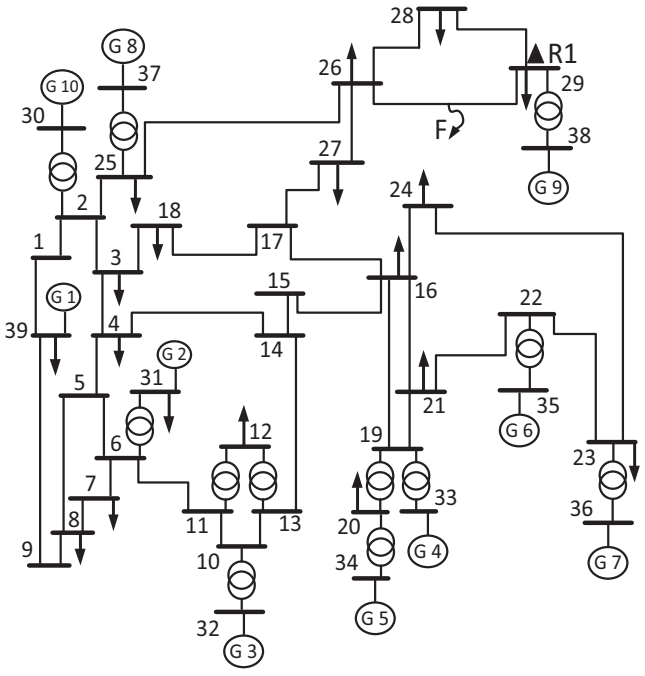

Fig. A. Single line diagram of IEEE 39-bus New-England test system.

References

[1] NERC Recommendations to August 14, 2003. Blackout—prevent and mitigate the impacts of future cascading blackouts; August 14, 2003. <www.NERC.com>.
[2] Garlapati S, Lin H, Heier A, Shukla SK, Thorp J. A hierarchically distributed non-intrusive agent aided distance relaying protection scheme to supervise Zone-3. Int J Electr Power Energy Syst 2013;30(50):42–9.
[3] Bakar AH, Yatim FM, Yusof S, Othman MR. Analysis of overload conditions in distance relay under severe system contingencies. Int J Electr Power Energy Syst 2010;32(5):345–50.
[4] Nayak PK, Pradhan AK, Bajpai P. Secured zone-3 protection during stressed condition. IEEE Trans Power Delivery 2015;30(1):89–96.
[5] Horowitz SH, Phadke AG. Third zone revisited. IEEE Trans Power Delivery 2006;21(1):23–9.
[6] Vaidyanathan R, Soman SA. Distance relay coordination considering power swings. In: Proc. int. conf. power syst. commun. syst. infrastructures for future; 2002 September 23.
[7] Khoradshadi-Zadeh H, Li Z. Adaptive load blinder for distance protection. Int J Electr Power Energy Syst 2011;33(4):861–7.
[8] Energy, G.E., D60 Line distance protection system instruction manual. <http://www.gedigitalenergy.com/products/manuals/d60/d60man-x2.pdf>; 2012.
[9] ABB. Line distance protection REL670 application manual. <https://library.e.abb.com/public/5b25d28d142a4ad0985bfe059141a566/1MRK506315-UEN_D_en_Application_manual__REL670_1.2.pdf>; 2015.
[10] Siemens. SIPROTEC- Distance protection 7SA6 manual, V4.7. <http://www.automation-berlin.com/downloads/siemens/energy_ptd/7SA6xx_Manual_A7_V047001_en.pdf>; 2011.
[11] Jin M, Sidhu TS. Adaptive load encroachment prevention scheme for distance protection. Electr Power Syst Res 2008;78(10):1693–700.
[12] Gunasegaran MK, Tan C, Bakar AH, Mokhlis H, Illias HA. Progress on power swing blocking schemes and the impact of renewable energy on power swing characteristics: a review. Renew Sustain Energy Rev 2015;31(52):280–8.
[13] IEEE Power System Relaying Committee. Power swing and out-of-step considerations on transmission line, PSRC WG D6. <http://www.pes-psrc.org>; July 2005.
[14] Fischer N. Application guidelines for power swing detection on transmission systems. In: IEEE power systems conference: advanced metering, protection, control, communication, and distributed resources; 2006 March 14. p. 159–68.
[15] Kang D, Gokaraju R. A new method for blocking third zone distance relays during stable power swings. IEEE Trans Power Deliv 2016;31(4):1836–43.
[16] Khoradshadi-Zadeh H. Evaluation and performance comparison of power swing detection algorithms. In: IEEE power engineering society general meeting; 2005 June 12. p. 1842–48.
[17] Rao JG, Pradhan AK. Power-swing detection using moving window averaging of current signals. IEEE Trans Power Delivery 2015;30(1):368–76.
[18] Jafari R, Moaddabi N, Eskandari-Nasab M, Gharehpetian GB, Naderi MS. A novel power swing detection scheme independent of the rate of change of power system parameters. IEEE Trans Power Delivery 2014;29(3):1192–202.
[19] Gautam S, Brahma SM. Out-of-step blocking function in distance relay using mathematical morphology. IET Gener Transm Distrib 2012;6(4):313–9.
[20] Chothani NG, Bhalja BR, Parikh UB. New support vector machine-based digital relaying scheme for discrimination between power swing and fault. IET Gener Transm Distrib 2014;8(1):17–25.
[21] Dubey R, Samantaray SR, Panigrahi BK, Venkoparao VG. Data-mining model based adaptive protection scheme to enhance distance relay performance during power swing. Int J Electr Power Energy Syst 2016;31(81):361–70.
[22] Jonsson M, Daalder JE. An adaptive scheme to prevent undesirable distance protection operation during voltage instability. IEEE Trans Power Delivery 2003;18(4):1174–80.
[23] Sharifzadeh M, Lesani H, Sanaye-Pasand M. A new algorithm to stabilize distance relay operation during voltage-degraded conditions. IEEE Trans Power Delivery 2014;29(4):1639–47.
[24] Abidin AF, Mohamed A. On the use of voltage stability index to prevent undesirable distance relay operation during voltage instability. In: IEEE Environment and Electrical Engineering (EEEIC), 2010 9th International Conference on 2010 May 16. p. 384–87.
[25] Nikolaidis VC. Emergency zone 3 modification as a local response-driven protection measure against system collapse. IEEE Trans Power Delivery 2016;31(5):2114–22.
[26] Song H, Lee B, Ajjarapu V. Control strategies against voltage collapse considering undesired relay operations. IET Gener Transm Distrib 2009;3(2):164–72.
[27] Zare J, Aminifar F, Sanaye-Pasand M. Synchrophasor-based wide-area backup protection scheme with data requirement analysis. IEEE Trans Power Delivery 2015;30(3):1410–9.
[28] Kundu P, Pradhan AK. Wide area measurement based protection support during power swing. Int J Electr Power Energy Syst 2014;31(63):546–54.
[29] Song H, Lee B, Ajjarapu V. Secured zone-3 protection during power swing and voltage instability: an on-line approach. IET Gener Transm Distrib 2017;11(2):437–46.
[30] Zadeh MD, Sidhu TS, Klimek A. Suitability analysis of practical directional algorithms for use in directional comparison bus protection based on IEC61850 process bus. IET Gener Transm Distrib 2011;5(2):199–208.

[31] Apostolov AP. High speed peer-to-peer communications based bus protection. In: IEEE power engineering society winter meeting, vol. 2; 2001. p. 693–98.
[32] Jafarian P, Sanaye-Pasand M. High-speed superimposed-based protection of series-compensated transmission lines. IET Gener Transm Distrib 2011;5 (12):1290–300.
[33] Power Systems Test Case Archive. <http://www.ee.washington.edu/research/pstca/>.
[34] DIgSILENT power factory, Version 14.1; 2008.